Direct Measurement of Small Ligand-Induced Conformational Changes in the Aspartate Chemoreceptor Using EPR†

Karen M. Ottemann,‡ Thorgeir E. Thorgeirsson,§,|| Andrew F. Kolodziej,‡,⊥ Yeon-Kyun Shin,§ and Daniel E. Koshland, Jr.*,‡

Department of Molecular and Cell Biology and Department of Chemistry, University of California, Berkeley, California 94720

Received February 6, 1998; Revised Manuscript Received March 27, 1998

ABSTRACT: Ligand-binding-induced conformational changes in the *Salmonella typhimurium* aspartate receptor were studied using spin-labeling electron paramagnetic resonance. Cysteine residues, introduced by site-directed mutagenesis at several positions in the aspartate receptor periplasmic domain, were used to attach covalently a thiol-specific spin label. The electron paramagnetic resonance spectra of these labeled proteins were obtained in the presence and absence of the ligand aspartate, and used to calculate the distance change between spin labels. The results support a model in which transmembrane signaling is executed by a combined movement of α helix 4 (which leads into transmembrane domain 2) relative to α helix 1 (connected to transmembrane domain 1), as well as a coming together of the two subunits. Ligand binding causes spin labels at position 39 and 179 (within one subunit) to move further from each other and spin labels at position 39 and 39′ (between two subunits) to move closer to each other. Both of these changes are very small—less than 2.5 Å. No similar changes were detected in any aspartate receptor samples solubilized in detergent, suggesting that the membrane is required for these conformational changes. This is the first case of physically measured ligand-induced changes in a full-length 1−2 transmembrane domain receptor, and the results suggest that very small ligand-induced movements can result in large effects on the activity of downstream proteins.

Transmembrane receptors are used to transmit information from the outside to the inside of a cell, but the exact protein conformational changes accompanying signal transduction events are unknown. Transmembrane receptors typically consist of an exterior stimulus recognition domain, an interior effector domain, and connecting transmembrane domains. Of these, the bacterial aspartate receptor (AR),[1] encoded by the *tar* gene and sometimes referred to as the Tar protein, falls into a class of receptors that contain one to two transmembrane (TM) domains per subunit. This class also includes the insulin receptor, the epidermal growth factor receptor, and the cytokine receptors.

The AR and its homologues allow bacteria to migrate toward nutrients and away from toxic substances (*1, 2*). The AR sits in the cytoplasmic membrane, with its ligand-binding domain in the periplasm. The structure of this isolated periplasmic domain has been determined, in the presence and absence of aspartate, to 1.85 and 2.2 Å resolution (*3, 4*). Each subunit consists of a four helix bundle, with TM domain 1 (TM1) connected to α helix 1 and TM domain 2 (TM2) connected to α helix 4 (Figure 1). The AR always exists as a homodimer, and the aspartate-binding pocket consists of residues from both subunits (*3, 5*). The AR regulates both a kinase cascade and its own methylation (*6*−*8*). The kinase cascade is composed of the CheA kinase, the CheW coupling protein, and the flagellar motor-regulator CheY. In the presence of aspartate, the rate of CheA autophosphorylation is reduced and, as a result, the amount of phospho-CheY is decreased 30-fold. These phosphorylation events lead to counterclockwise flagellar rotation and smooth swimming. Aspartate binding also increases the methylation of the receptor, which is required for receptor down regulation.

The ligand-generated conformational changes and mechanism of transmembrane signaling in the AR are not yet known. The first experiments to measure the structural effects of ligand on the AR compared disulfide bond formation rates in the presence and absence of aspartate (*9*). Results from these and subsequent experiments showed that aspartate triggered global changes in the receptor structure (*9*−*11*). This is also true of the related ribose and galactose receptor (Trg) (*12*). These conformational changes induced by ligand binding include bringing the two subunits of the AR closer to each other, as well as global movements, but did not reveal the precise nature of the ligand-induced movements.

† Research supported by NIH Grant DK09765 and the W.M. Keck Foundation to DEK, NIH Grant GM51290 and a Searle Scholarship to Y.-K.S., and Postdoctoral Fellowships from the American Cancer Society to K.M.O., and the Damon Runyon−Walter Winchell Cancer Fund to A.F.K.

* Corresponding author: 229 Stanley Hall, Berkeley, CA 94720-3206. E-mail: dek@uclink4.berkeley.edu.

‡ Department of Molecular and Cell Biology.

§ Department of Chemistry.

|| Present address: Decode Genetics, Lynghals 1, 110 Reykjavik, Iceland.

⊥ Present address: EPIX Medical, Inc. 71 Rogers St., Cambridge, MA 02142-1118.

[1] Abbreviations: EPR, electron paramagnetic resonance; DTT, dithiothreitol; MTSSL, (1-oxyl-2,2,5,5-tetramethylpyrroline-3-methyl)-methanethiosulfonate spin label; AR, aspartate receptor; TM, transmembrane; OG, *n*-octyl β-D-glucopyranoside.

S0006-2960(98)00305-5 CCC: $15.00
Published on Web 05/02/1998

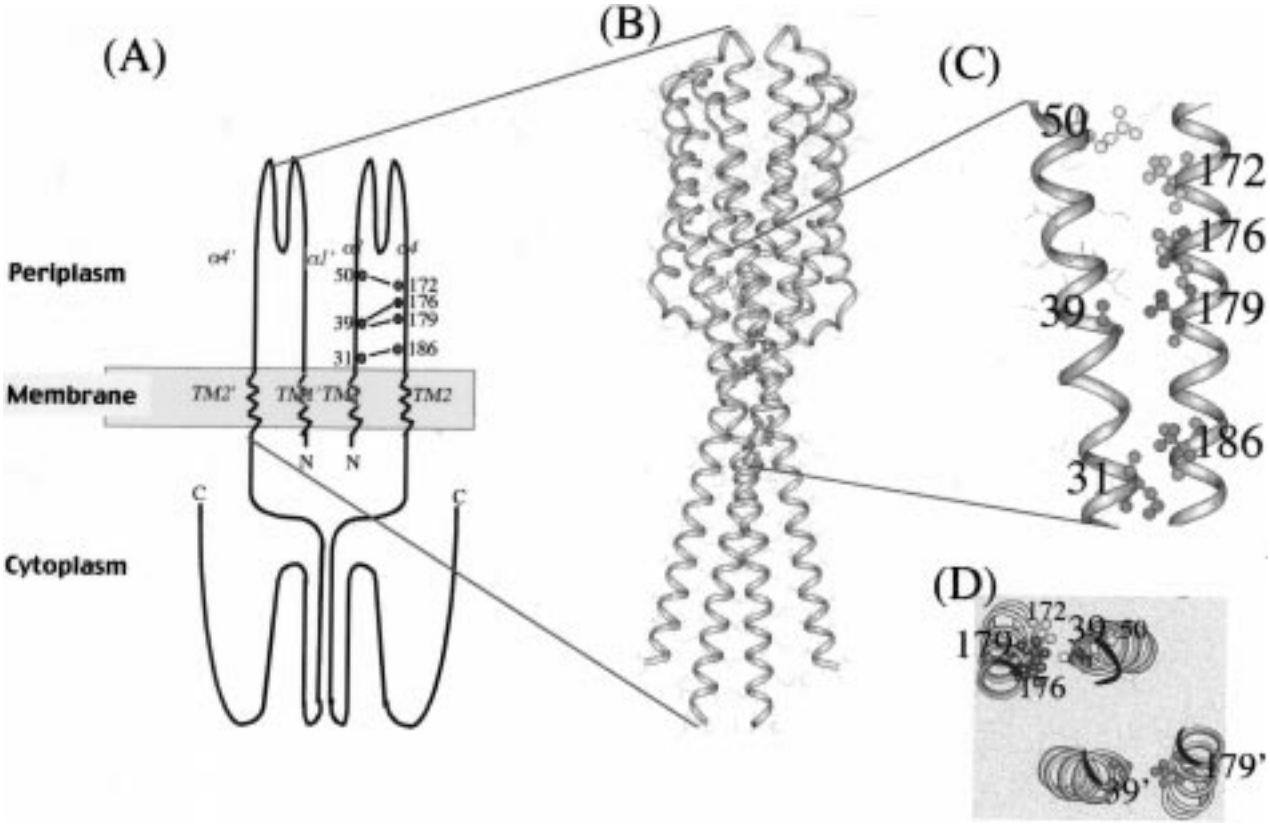

FIGURE 1: Spin-labeled sites in the aspartate receptor. (A) A schematic of the AR, showing the periplasmic ligand binding, transmembrane (zigzag), and cytoplasmic domains. The periplasmic helices α1 and α4 are labeled, as are TM1 and TM2; in the second subunit these are denoted by prime signs. The locations of spin labels, analyzed in pairs, are shown by large dots, with connecting lines. The pairs of residues from top to bottom are: 50−172 (both green), 39 (purple)−176 (blue), 39−179 (both purple), and 31−186 (both red). (B) The crystal structure of the periplasmic ligand binding domain, with modeled TM helices (*3, 14*). The location of the spin labels are shown as ball-and-stick residues. (C) Closeup view of the locations of spin labels on helices α1 and α4. (D) View from the membrane of the periplasmic domain. Amino acids used for spin label attachment are shown as balls and sticks. Amino acids 39′ and 179′ are shown in pink.

Crystal structures of the periplasmic ligand-binding domain in the presence and absence of aspartate (*3, 4*) have also not exposed the nature of the aspartate-induced motions. Some analyses of these data found evidence that ligand-binding initiates intersubunit motions, consisting of a piston-type movement of α helix 1 relative to α helix 4 (*13, 14*). That this type of movement could allow transmembrane signaling was supported by a separate analysis using biochemical results from truncated receptors (*15*). Other analyses of these same crystallographic data, however, found intersubunit motions (*3, 4, 16*). Aspartate binding led to a decrease in the water-accessible surface area of the periplasmic domain, consistent with an overall tightening of the structure (*4*). Furthermore, both the full-length receptor and the isolated periplasmic domain exhibit negative cooperativity: the affinity for the first aspartate is much greater than that for the second aspartate molecule (*17*). This allosteric behavior is very sensitive to the composition of the subunit interface and is thought to result from first-aspartate-induced changes in the conformation of the second aspartate-binding site (*18*). These results indicate that aspartate is able to cause intersubunit conformational changes, but the relevance of these motions to TM signaling is not clear.

What motions does aspartate instigate in the AR? To understand how aspartate binding results in transmembrane signaling, we sought to precisely define the ligand-triggered movements in the full-length, membrane-bound AR. In this work, we report a spin-labeling electron paramagnetic resonance (EPR) characterization of these movements. The experimental strategy was to site-specifically place two nitroxide spin labels into double cysteine mutants of the AR (*19, 20*) and measure the distances between these label pairs using a dipolar EPR method (*21*). Recently, the dipolar EPR method to measure interspin distances has been systematically tested (*21*) and improved (*22*), and it has proven to be particularly powerful in determining functionally important protein conformational changes in many biological systems (*23*−*26*). By placing spin labels in the periplasmic domain of the AR, we were able to measure aspartate-induced protein conformational changes; these may well constitute the transmembrane-signaling motions.

MATERIALS AND METHODS

Protein Expression and Purification. To create cysteine-containing mutant AR, the gene encoding the wild-type AR (*tar*$_S$) was mutated using site-directed mutagenesis as described (*18*). The AR contains no endogenous cysteines, and thus, the introduced cysteines are the only ones. Plasmid pEMBLtarS (*9*) was used to prepare uracil-enriched ssDNA. Oligonucleotides were from the U. C. Berkeley DNA synthesis facility. Mutations were verified using dsDNA Cycle Sequencing (Gibco). Wild-type and mutant proteins were expressed in *E. coli* strain HCB721 [Δ(*tsr*)7021 *trg*::Tn10 Δ(*cheA-cheY*)::XhoI(*Tn5*) (*27*)], which lacks all chemotaxis genes except *cheZ*.

AR was purified as described, by first preparing bacterial membranes (*17*), with the inclusion of 10 mM dithiothreitol (DTT), followed by solubilization with *n*-octyl β-D-glucopyranoside (OG) (*28, 17*). After ammonium sulfate precipitation, the protein was applied to an ω-aminooctyl agarose (Sigma) and eluted with a linear gradient of 0 to 400 mM NaCl. AR containing fractions were pooled and concentrated 30−50-fold using centriprep 30 (Amicon). This yielded protein that was 90−95% pure, as estimated using SDS−PAGE.

Reaction with MTSSL and Reconstitution into E. coli Membranes. The protein concentration was next estimated by the method of Bradford (*29*) (Bio-Rad) using either amino-acid-analyzed AR or bovine serum albumin as a standard. Two to three milligrams of protein was then passed over a Sephadex G25 gel filtration column pre-equilibrated with final buffer (FB) [50 mM Tris pH 8.0 at 4 °C, 10% (w/v) glycerol, 5 mM EDTA, 1% OG] to remove the DTT. Eluted AR-containing fractions were immediately mixed with a 5-fold molar excess (1-oxyl-2,2,5,5-tetramethylpyrroline-3-methyl)methanethiosulfonate spin label (MTSSL) per cysteine (Reanal, Hungary, dissolved in acetonitrile at a concentration of 50 mM) and reacted in the dark with gentle agitation for 14−18 h at 4 °C. Wild-type AR was reacted with a 2−5-fold excess MTSSL/mol protein.

After reaction, excess MTSSL was removed by gel filtration (as above, equilibrated with FB pH 7.5 at 4 °C), and the AR was concentrated by ultrafiltration in centricon 30 (Amicon) to 5−10 mg/mL. An aliquot of this was saved to be analyzed as the OG detergent sample. The remainder was reconstituted into total *E. coli* membranes as follows. An *E. coli* total lipid extract (Avanti) was prepared by reversed-phase evaporation (*30*) and mixed with spin-labeled AR at a 12-fold (weight) excess and 1/10 volume of 10% OG. This was then quickly frozen in liquid nitrogen, thawed at 37 °C, and dialyzed to remove the OG in 10 kDa cutoff slidealyzers (Pierce) against 500−1000 vol of 50 mM sodium phosphate buffer, pH 7.0, 1 mM EDTA (reconstitution buffer), and 70 μg/mL PMSF at 4 °C.

For mixing of labeled AR with unlabeled wild-type receptor, equimolar amounts of each, in OG, were mixed together and allowed to incubate for 30−60 min at room temperature (*5*). These samples were then reconstituted into *E. coli* phospholipids as above.

EPR Spectroscopy and Interspin Distance Calculations. A total of 4.5 μL of labeled AR (at ∼100 μM) was mixed with either 0.5 μL of reconstitution buffer or 100 mM L-aspartate in the same buffer, and placed in quartz capillaries. EPR spectra were collected using a Bruker ESP 300E spectrometer equipped with a loop-gap resonator (Medical Advances, Milwaukee, WI) and a low-noise amplifier (Miteq, Hauppauge, NY). Room-temperature spectra were collected using 1 mW microwave power and a modulation amplitude of 1 G. Low-temperature spectra were collected at 140 K using 8 μW microwave power and a modulation amplitude of 2 G. Spin concentrations were determined by comparing doubly integrated spectra to that of a TEMPO standard solution. The spin labeling was quantitative (100 ± 10%) after correction for the nonspecific labeling seen in wild-type AR.

A Fourier transform method was used to deconvolute the biradical EPR spectrum into the dipolar broadening function and the monoradical spectrum. This was used to determine the spin−spin distances as described (*21*).

Protein Quantification. The AR protein standard was a purified sample that had been dialyzed exhaustively against 10 mM Tris and 0.02% SDS and sent to the U. C. Davis Protein Structure Laboratory for amino acid analysis. The spin-labeled AR samples were quantified as described (*18*) using gel electrophoresis, scanning with a flat bed scanner, and quantification, by comparison to the known standard, using the public domain NIH Image program (developed at the U.S. National Institutes of Health and available on the Internet at http://rsb.info.nih.gov/nih-image/).

Phosphorylation Assays. Salmonella typhimurium CheA, CheW, and CheY were purified as described from plasmids pMO4, pME106, and pME124, respectively (*31*−*33*). The in vitro phosphorylation assay (*34*) was performed with 114 pmol of CheY, 8.8 pmol of CheA, 21−42 pmol of CheW, 100 pmol of labeled AR, 5 mM $MgCl_2$, 50 mM KCl, 50 mM Tris pH 7.5, and ±2 mM aspartate in a volume of 10−12 μL. After equilibration at room temperature for 45−60 min, the reaction was initiated by adding γ-labeled [^{32}P]ATP (Dupont, 6000 Ci/mmol) (5000 cpm/pmol) to 100 μM and then terminated after 45 s by addition of an equal volume of 4× SDS sample buffer (*35*). Triplicate 3−5 μL aliquots of each sample were loaded on 16% SDS−PAGE gels, and the relative radioactivity of each band was quantitated using a phosphorimager (Molecular Dynamics). Band volumes were normalized to that of the no-receptor reaction.

RESULTS

Construction of Receptors with Spin Labels and Spectral Analysis. To characterize ligand-induced motion(s) in the AR, we placed pairs of spin labels at several locations in the periplasmic domain of the receptor (Figure 1). Because the molecular structure of the periplasmic domain is known (*3, 4*), spin labels were positioned to favor the monitoring of intra- or intersubunit interactions that might be involved in signal transmission. Spin labels were thus placed, two per receptor subunit, at positions 50−172, 39−176, 39−179, and 31−186 (the first number indicates the residue position on α helix 1 and the second number refers to the residue position on α helix 4).

The cysteine-mutated ARs were purified, reacted with MTSSL and reconstituted into purified *E. coli* membranes. The room-temperature EPR spectra of the spin-labeled AR were collected, and the spectral line shapes were analyzed qualitatively using two criteria. First, spectra were compared to ascertain whether the addition of aspartate resulted in any changes in the spectral line shape; changes would be indicative of measurable ligand-induced structural changes. Second, the spectrum of each doubly spin-labeled AR was examined for evidence of spectral line broadening. In both the absorbance and first derivative spectra, line broadening is typified by the spectral components exceeding the outermost hyperfine splitting. This is best evaluated by comparison of an interacting spectrum with its two component, singly labeled, noninteracting spectra. This can be seen graphically as the outermost edges of the spectra extending further than 35 G from the center of the spectrum (Figure 2). At room temperature, spectral line broadening is due to complex combinations of exchange interactions, alterations

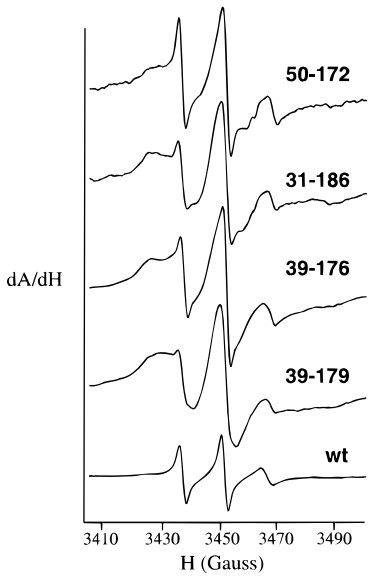

FIGURE 2: Room temperature EPR spectra of doubly spin-labeled AR. Shown are first-derivative EPR spectra for each spin-labeled double AR mutant and wild-type (wt) AR. For the cysteine variants, the spectra are normalized to the peak height. Also shown is the spectrum due to nonspecific labeling of the wild-type receptor (wt), scaled to represent the ratio of spin/protein. The sweep width is 150 G. The *x*-axis is H (Gauss) with tick marks denoting intervals of 20 G; the *y*-axis is dAbsorbance/d*H*.

in molecular tumbling and magnetic dipole interactions (*36*). These interactions can be dissected in motionally frozen samples because the major source of spectral line broadening in this state is spin−spin dipolar interaction which can be related directly to the distance between the spin labels (*21*). Thus, we used room-temperature analysis to detect aspartate-induced spectral changes, frozen sample data to determine the extent of dipole−dipole interactions, and from this the spin−spin distance.

Aspartate Binding Causes Small but Reproducible Changes in the Receptor. Room-temperature EPR spectra were obtained of the spin-labeled AR samples (Figure 2). All doubly labeled AR displayed spectral line broadening, suggesting that the two labels might be close enough for electron spin−spin interactions. When aspartate was added to the Q50C−S172C, S31C−D186C, and G39C−Y176C samples, there were no spectral changes, indicating that significant changes in spin-probe mobility or spin−spin interactions were not detectable with these mutants. One of the labeled receptors, AR G39C−T179C, did show a ligand-induced change in its spectra (Figure 3, top spectra). Although the change is small, these results were repeated with five separately purified and labeled AR G39C−T179C protein preparations, and aspartate binding resulted in similar spectral changes in all cases. No spectral changes were detected in any of these labeled AR samples when they were in OG detergent, suggesting that conformational changes are enhanced by lipids. Thus, it appears that the 39−179 region of the AR moves upon aspartate binding.

Wild-type AR (with no cysteines) was also found to be labeled by MTSSL (0.5 labels/subunit), but at a level that was only 25% of that observed for doubly labeled receptors (Figure 2). This apparently nonspecific labeling did not show any spin−spin interaction or aspartate-induced spectral changes.

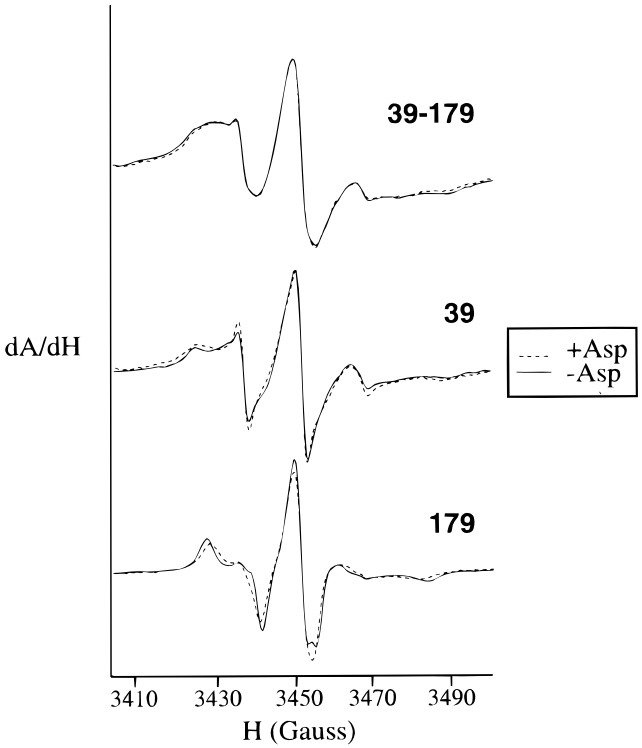

FIGURE 3: Room-temperature spectra of AR labeled at positions G39C, T179C, and G39C−T179C. First-derivative EPR spectra for each spin-labeled AR in the presence (dotted line) and absence (solid line) of aspartate. The spectra are normalized to peak height. The sweep width is 150 G.

To discern if the spectral change in labeled AR G39C−T179C was due to changes between 39 and 39′, 179−179′, 39−179′, or 39′−179, room temperature spectra of AR with labels only at positions G39C or T179C were obtained (Figure 3). In spin-labeled T179C, there was no evidence for spin−spin interactions, consistent with these two positions being far from each other. In the presence of aspartate, the spectrum narrowed (Figure 3). This type of change is compatible with this spin label becoming more mobile. In the labeled G39C, the spectrum was broadened, consistent with the possibility of spin−spin interactions between these two sites (Figure 3). The AR G39C spectrum broadened further upon aspartate addition; one explanation for this is that the spin labels on positions 39 and 39′ approach each other (Figure 3) (this is further examined in the frozen state; see below). In the doubly labeled AR G39C−T179C, in contrast, aspartate caused the spectrum to narrow. The fact that the 39−39′ broadening is overshadowed in this sample indicates that spin labels at positions 39−179, 39−179′, or 39′−179 interact more strongly than those at 39−39′. The aspartate-induced narrowing in G39C−T179C may indicate that these interacting spin labels moved further apart on addition of aspartate (Figure 3). Although the origins of the aspartate-induced spectral changes must be further examined to separate mobility changes versus changes in spin−spin interactions (see below), it appears that the spectral change in labeled AR G39C−T179C reflects a combined movement of 39−39′ closer to each other, and a movement between 39−179, 39−179′, or 39′−179 further apart.

The Spin−Spin Interaction and Change in AR G39C−T179C Is Intrasubunit. Each doubly labeled AR contains four spin labels per dimer, and thus spin−spin interactions

could result from several possible dipolar couplings. To determine if the interactions in labeled AR G39C−T179C were due to intra- or intersubunit interactions, we mixed unlabeled wild-type AR (at a 1:1 ratio) with labeled AR G39C−T179C or labeled AR G39C. Exchange of the receptor subunits dilutes the labeled AR such that only 25% of the population contain labels on both subunits. These samples were then reconstituted into phospholipid vesicles, and EPR spectra were recorded in the presence and absence of aspartate. In both cases, dilution with wild-type reduced the total spin concentration by 2-fold. In the case of labeled AR G39C, the dilution decreased the broadening of the spectral line, consistent with the spin−spin interactions arising from intersubunit interactions. In contrast, when labeled AR 39C−T179C was diluted, the spectral line shape did not change, indicating that the spin−spin interactions seen in labeled AR G39C−T179C arose exclusively from interactions within one subunit. Additionally, the magnitude of the aspartate-induced spectral change in labeled AR G39C−T179C was the same with and without dilution by wild-type, indicating that this change is the result of alterations within the same subunit. These results indicate that the G39C−T179C EPR spectral changes most likely reflect changes occurring within one subunit, with little contribution from the changes in the intersubunit 39−39′ distance.

Spin-Labeled Aspartate Receptors Are Functional. The lack of a detectable change in the majority of labeled AR can be explained in several possible ways: the labeling of the receptor inactivated it such that it no longer bound or responded to aspartate, the change is below the detection limit, the spin labels are insensitive to the conformational change, or there is no change. To exclude the possibility that labeling inactivated the receptor, we performed in vitro functional assays on the labeled AR. AR normally regulates a kinase, CheA, in response to aspartate (*8*), and the CheA kinase phosphorylates a second protein, CheY. In the presence of liganded receptor, the phosphorylation rate of CheA decreases, and thus the amount of CheY-phosphate decreases. CheY phosphorylation was measured with the spin-labeled AR; all receptors were able to regulate the amount of CheY-phosphate in response to aspartate (Figure 4). In addition, spin labeling of wild-type AR did not alter its function (Figure 4). These results suggest that the labeled receptors are functional and that lack of observed change is not due to loss of functionality.

39 Moves Closer to 39′ but Further from 179. To separate spin−spin interactions from other relaxation mechanisms, especially molecular tumbling, we collected EPR spectra at low temperature (140 K). At room temperature, electron spin−spin interaction broadening is the result of an intricate interplay of exchange interactions, magnetic dipolar interactions, and molecular tumbling that are difficult to analyze quantitatively. At low temperatures, however, the dipolar interaction is the dominant source of spectral broadening; this allows determination of spin−spin distances between 8 and 25 Å (*21*). When EPR spectra were recorded at 140 K, again the spectra of labeled AR G39C broadened and the spectra of labeled AR G39C−T179C narrowed in the presence of aspartate (Figure 5). Labeled AR T179C did not have any aspartate-induced spectral changes at 140 K (Figure 5), consistent with the labeled T179C room-temperature spectral changes arising from alterations in spin mobility. Thus, because they persist in the frozen state, the aspartate-induced spectral changes in labeled AR G39C and labeled AR G39C−T179C result from changes in spin−spin interactions due to interspin distance changes.

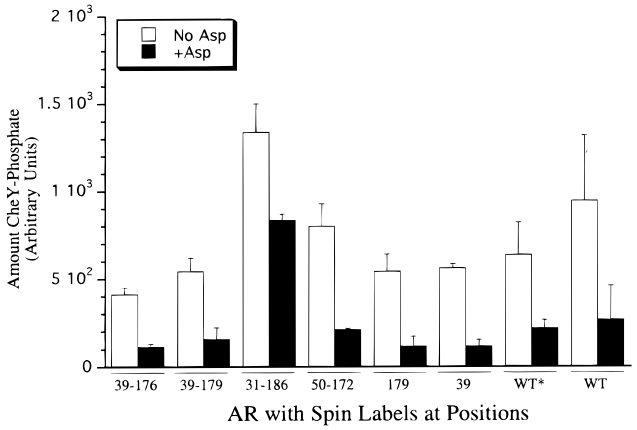

FIGURE 4: Spin-labeled receptors are able to regulate CheY-phosphate formation. The amount of CheY-phosphate is plotted for each mutant, and spin-label-reacted (wt*) and unlabeled wild-type AR in the absence (open bars) and presence of aspartate (filled bars). The *y*-axis is arbitrary absorbance units. Results given here are representative of two to three separate experiments.

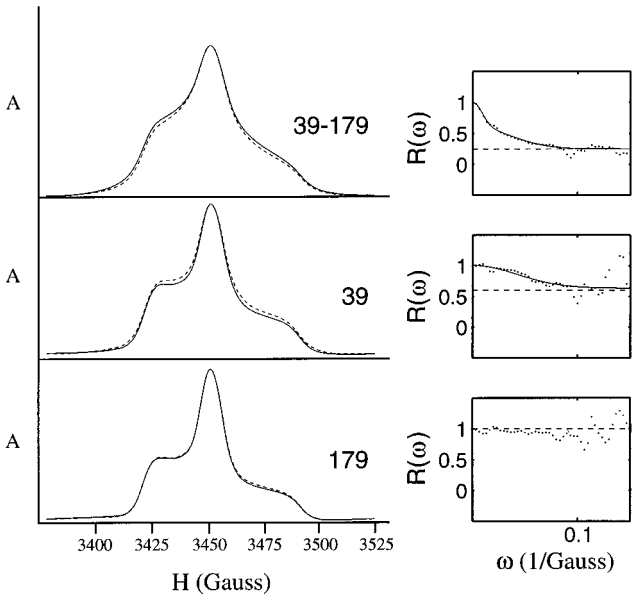

FIGURE 5: Low-temperature EPR spectra and Fourier deconvolution analysis for spin-labeled AR mutant proteins. (Left panel) Low-temperature absorbance (integrated) spectra for the doubly labeled mutants in the presence (dashed line) and absence (solid line) of aspartate. The *x*-axis is H (Gauss) with tick marks denoting intervals of 25 G; the *y*-axis is arbitrary absorbance units. (Right panel) The real part of the dipolar broadening function (in Fourier space) obtained when the spectra in the left side were used as the interacting spectra, and the spectrum of AR T179C was used as the noninteracting spectrum. The data are fit to a sum of 2 Gaussians. In the Fourier analysis, the fraction of monoradical impurities appears as a constant *y*-axis offset (*21, 25*). From these *y*-axis offsets of the dipolar broadening functions, it can be seen that the monoradical fraction consists of 30% in 39−179, 60% in 39, and 100% in 179. This is as expected from the protein and spin quantitation, and the contribution of the nonspecific labeling of wild-type AR. The interspin distances were calculated from dipolar broadening functions after inverse Fourier transform.

Fourier deconvolution analysis by the method of Rabenstein and Shin (*21*) was performed on labeled AR G39C,

AR T179C, and AR G39C−T179C (Figure 5). The distance between the two spin label nitroxide groups of labeled AR G39C was ∼15 Å in the absence of aspartate. This distance decreased in the presence of aspartate by ∼1 Å. This measurement was repeated on four separate spin-labeled AR G39C samples. The nitroxide−nitroxide distance of ∼12 Å in labeled AR G39C−T179C increased by ∼0.5 Å in the presence of aspartate. This measurement was repeated on five distinct spin-labeled AR G39C−T179C samples; thus, although the distance change is small, it is very reproducible. Furthermore, these distances are consistent with those measured in the AR high-resolution structure (*3, 14*): 39−39′ (α carbon to α carbon) distance was 11.37 Å, the 39−179 distance was 5.09 Å, and the 39−179′ distance was 14.65 Å.

DISCUSSION

We found that ligand binding initiates several measurable events in the AR. First, spin labels at positions 39 and 39′ move ∼1 Å closer to each other, consistent with the two subunits of the receptor becoming closer. Additionally, positions 39 and 179 (within one subunit) moved further from each other by ∼0.5 Å upon ligand binding, suggesting that at least some positions on α helix 4 move further from positions on α helix 1. Last, a spin label on position 179 was more mobile in the presence of aspartate, suggesting that α helix 4 in the vicinity of position 179 is less constrained in the presence of aspartate.

These observed distance changes are small, but reproducible. The EPR dipolar method measures the distance between the unpaired electrons localized at the ends of the two nitroxide side chains. Unless both of the nitroxide side chains are geometrically fixed in three-dimensional space (*22*), the flexibility of the nitroxide side chain results in a distribution of interspin distances. We think this variability constitutes the major uncertainty in the EPR distance measurement and may also make detection of very small changes challenging. Both an experimental measurement (*21*) and a theoretical simulation (*37*) based on well-defined α-helical peptides predicted that the uncertainty due to this side-chain flexibility may be as much as 2.5 Å (*21, 37*). For the AR, the distance changes measured with EPR are smaller than the uncertainty of the measurement. However, since these aspartate-induced movements were observed with 4−5 separate protein preparations, we believe they are real and representative of the actual-ligand induced motions. Instead of assigning a numerical value to the measured distance changes, we would prefer to interpret these changes qualitatively as small changes less than 2.5 Å.

Surprisingly, aspartate did not alter the spectra of most spin labels on the AR. Nonchanging spectra include those of one spin label/subunit, located on either α helix 1 or α helix 4, as well as those of two spin labels per subunit (Figures 2 and 3 and data not shown). Interestingly, results from crystallographic studies have shown that movements of α-helical main-chain residues up to 1.5 Å can be tolerated without movement of the side chains (*38, 39*). Thus, aspartate could induce a 1.5 Å movement of the receptor main-chain atoms with a concomitant adjustment of the side-chain atoms to retain the same or similar positions. This is true for the shear-type motions that occur between two α helices (*39*) and is consistent with the piston-type motion hypothesized for the AR (*13, 40*). One possible explanation for the lack of aspartate-induced differences in the spectra of labeled 39−176, 50−172, and 31−186 is that the backbone movements are dampened by accompanying side-chain adjustments, and spectrally there is no visible change in the presence of ligand.

Ligand binding, as described here, leads to small structural changes both within one subunit and between two subunits of the periplasmic domain of the AR. We presume these small changes are translated into a large amplification of the phosphorylation cascade regulated by the receptor cytoplasmic domain, but the exact nature of these cytoplasmic events remains to be discovered. Recently, Liu et al. postulated the formation of large multicomponent complexes composed of the isolated AR cytoplasmic signaling domain, CheA and CheW (*41*). We found no evidence for such complexes in our experiments with the full receptor, and furthermore, the dilution experiments with unlabeled wild-type AR strongly support the conclusion given here that conformational changes occur within one subunit. It is possible that ligand binding leads to small periplasmic conformational changes that, in turn, bring about changes in the AR multimeric state; that will be a subject for future study but does not alter the conclusion that aspartate binding causes small conformational changes in the periplasmic domain of the intact receptor as shown here.

The region of AR 39−179 (see Figure 1) appears to be conformationally sensitive to the effects of aspartate. Ligand binding increased the mobility of labeled T179C. Similarly, position 180 became solvent accessible in the presence of aspartate (*42*) consistent with this region being able to move in response to ligand. Labeled residue 39 was the only residue on α helix 1 whose spectrum altered upon ligand binding (Figure 3 and data not shown for positions 50 and 31). In this region of the protein, therefore, the amino acid side chains may be less constrained and, thus, more able to move in response to aspartate.

Experiments in which disulfide bonds were used to lock the AR and the related Trg receptor into specific conformations have helped identify which helices move. Results from these types of studies have shown that numerous disulfide bonds along the α helix 1−α helix 1′ interface do not prevent transmembrane signaling (*9, 43−45*). The majority of disulfide bonds between α helix 1 and α helix 4 (intrasubunit) prohibit transmembrane signaling (*9, 12, 44−46*). Specifically, disulfide bonds between positions 39−179 perturb the AR conformation such that it is more like the aspartate-bound state as assayed by both in vitro phosphorylation and methylation (*46*) and in vivo methylation (*45*). These results support the importance of movements between α helix 1 and α helix 4 during transmembrane signaling and further highlight the significance of residues 39 and 179 in facilitating this motion.

While it appears from the crystallographic and biochemical data that both inter- and intrasubunit ligand-induced movements can occur, there is evidence that only one type is sufficient for transmembrane signaling. An AR variant, consisting of only one cytoplasmic domain but a normal dimeric periplasmic domain, was able to carry out transmembrane signaling (*15*). This suggested that ligand-induced motions can be propagated in one cytoplasmic domain, a

result that was confirmed subsequently with genetic experiments (*47*, *48*). A different AR variant, lacking transmembrane domains and not localized to the membrane (soluble), was also able to transmit ligand-induced signals (*49*). This suggests that relative pushing and pulling of the receptor in/out of the membrane is not required for signal transduction. Because of these results and the observation that the soluble AR is only partially functional, it was suggested that the wild-type AR transmembrane-signaling motion consists of both an intrasubunit motion and an intersubunit movement (*49*). Thus, both movements may contribute to the transmembrane signal, but either is sufficient; this is consistent with our quantitative EPR measurements of both inter- and intrasubunit motions.

These studies extend the utility of EPR spectroscopy by identifying and characterizing a movement that appears to be <2.5 Å. EPR spectroscopy has been used in several systems to characterize protein dynamics. Qualitative examples of this include oxygen-induced conformational changes in hemoglobin (*50*), estimation of intersubunit distances in both glyceraldehyde-3-phosphate dehydrogenase (*51*) and helix-loop-helix peptides (*52*), and characterization of light-induced changes in rhodopsin (*53*). Quantitatively, EPR has been used to characterize a 14−16 Å interhelix distance in lactose permease (*54*), a 5 Å light-induced motion in the cytoplasmic interhelical loops of bacteriorhodopsion (*26*) and a 6 Å change upon maltose binding in the maltose binding protein (*25*). Our studies have shown that the EPR is useful for identifying and characterizing even smaller protein motions.

What is the ligand-induced motion in the AR? In the full-length membrane-bound receptor, both intra- and intersubunit movements occur upon aspartate binding. These motions are small: less than 2.5 Å. Ligand binding initiates a movement of α helix 4 relative to α helix 1 within one subunit; this motion is consistent with a piston-type action of α helix 4 as has been postulated previously (*13*, *14*, *40*). Additionally, ligand binding causes the two subunits of the AR to come closer together, corroborating evidence from disulfide bond formation, and X-ray crystallography (*4*, *9*, *11*). This study shows that very small conformational changes occur upon aspartate binding, yet binding of aspartate causes dramatic changes in both the receptor-mediated phosphorylation and methylation of the receptor. This phenomenon thus illustrates the power of amplification through the sensitivity of enzymes.

ACKNOWLEDGMENT

The authors would like to thank Joe Falke for the modeled TM domain crystal structure, Mike Surette and Jeff Stock for the CheA, CheW and CheY plasmids, and Mike Oh and Ryan Louie for technical assistance.

REFERENCES

1. Adler, J. (1966) *Science 153*, 708−16.
2. Stock, J. B., and Surette, M. G. (1996) in *Escherichia coli and Salmonella: Cellular and Molecular Biology* (Neidhardt, F. C., Curtiss, R. I., Ingraham, J. L., Lin, E. C. C., Low, K. B., Magansanik, B., Reznikoff, W. S., Riley, M., Schaechter, M., and Umbarger, H. E., Eds.) Vol. 1, pp 1103−1129, ASM Press, Washington DC.
3. Milburn, M. V., Prive, G. G., Milligan, D. L., Scott, W. G., Yeh, J., Jancarik, J., Koshland, D. E., Jr., and Kim, S. H. (1991) *Science 254*, 1342−1347.
4. Yeh, J. I., Biemann, H. P., Prive, G. G., Pandit, J., Koshland, D. E., Jr., and Kim, S. H. (1996) *J. Mol. Biol. 262*, 186−201.
5. Milligan, D. L., and Koshland, D. E., Jr. (1988) *J. Biol. Chem. 263*, 6268−6275.
6. Goy, M. F., Springer, M. S., and Adler, J. (1977) *Proc. Natl. Acad. Sci. U.S.A. 74*, 4964−4968.
7. Springer, W. R., and Koshland, D. E., Jr. (1977) *Proc. Natl. Acad. Sci. U.S.A. 74*, 533−537.
8. Hess, J. F., Bourret, R. B., and Simon, M. I. (1988) *Nature 336*, 139−143.
9. Falke, J. J., and Koshland, D. E., Jr. (1987) *Science 237*, 1596−1600.
10. Lynch, B. A., and Koshland, D. E., Jr. (1991) *Proc. Natl. Acad. Sci. U.S.A. 88*, 10402−10406.
11. Chen, X., and Koshland, D. E., Jr. (1997) *Biochemistry 36*, 11858−11864.
12. Hughson, A. G., and Hazelbauer, G. L. (1996) *Proc. Natl. Acad. Sci. U.S.A. 93*, 11546−11551.
13. Lynch, B. A., and Koshland, D. E., Jr. (1992) *FEBS Lett. 307*, 3−9.
14. Chervitz, S. A., and Falke, J. J. (1996) *Proc. Natl. Acad. Sci. U.S.A. 93*, 2545−2550.
15. Milligan, D. L., and Koshland, D. E., Jr. (1991) *Science 254*, 1651−1654.
16. Kim, S. H. (1994) *Protein Sci. 3*, 159−165.
17. Biemann, H. P., and Koshland, D. E., Jr. (1994) *Biochemistry 33*, 629−634.
18. Kolodziej, A. F., Tan, T., and Koshland, D. E., Jr. (1996) *Biochemistry 35*, 14782−14792.
19. Miick, S. M., Martinez, G. V., Fiori, W. R., Todd, A. P., and Millhauser, G. L. (1992) *Nature 359*, 653−655.
20. Millhauser, G. L. (1992) *Trends Biochem. Sci. 17*, 448−452.
21. Rabenstein, M. D., and Shin, Y. K. (1995) *Proc. Natl. Acad. Sci. U.S.A. 92*, 8239−8243.
22. Hustedt, E. J., Smirnov, A. I., Laub, C. F., Cobb, C. E., and Beth, A. H. (1997) *Biophys. J. 72*, 1861−1877.
23. Farrens, D. L., Altenbach, C., Yang, K., Hubbell, W. L., and Khorana, H. G. (1996) *Science 274*, 768−770.
24. Yang, K., Farrens, D. L., Altenbach, C., Farahbakhsh, Z. T., Hubbell, W. L., and Khorana, H. G. (1996) *Biochemistry 35*, 14040−14046.
25. Hall, J. A., Thorgeirsson, T. E., Liu, J., Shin, Y. K., and Nikaido, H. (1997) *J. Biol. Chem. 272*, 17610−17614.
26. Thorgeirsson, T. E., Xiao, W., Brown, L. S., Needleman, R., Lanyi, J. K., and Shin, Y.-K. (1997) *J. Mol. Biol. 273*, 951−957.
27. Wolfe, A. J., Conley, M. P., and Berg, H. C. (1988) *Proc. Natl. Acad. Sci. U.S.A. 85*, 6711−6715.
28. Foster, D. L., Mowbray, S. L., Jap, B. K., and Koshland, D. E., Jr. (1985) *J. Biol. Chem. 260*, 11706−11710.
29. Bradford, M. M. (1976) *Anal. Biochem. 72*, 248−254.
30. Szoka, F., Jr., and Papahadjopoulos, D. (1978) *Proc. Natl. Acad. Sci. U.S.A. 75*, 4194−4198.
31. Stock, A., Koshland, D. E., Jr., and Stock, J. (1985) *Proc. Natl. Acad. Sci. U.S.A. 82*, 7989−7993.
32. Stock, A., Mottonen, J., Chen, T., and Stock, J. (1987) *J. Biol. Chem. 262*, 535−537.
33. Stock, A., Chen, T., Welsh, D., and Stock, J. (1988) *Proc. Natl. Acad. Sci. U.S.A. 85*, 1403−1407.
34. Ninfa, E. G., Stock, A., Mowbray, S., and Stock, J. (1991) *J. Biol. Chem. 266*, 9764−9770.
35. Ausubel, F. M., Brent, R., Kingston, R. E., Moore, D. D., Seidman, J. G., Smith, J. A., and Struhl, K. (1995) in *Current Protocol* (Janssen, K., Ed.) John Wiley and Sons.
36. Eaton, G. R., and Eaton, S. S. (1989) in *Biological Magnetic Resonance, Vol. 8: Spin Labeling Theory and Applications* (Berliner, L. J., and Reuben, J., Eds.) Vol. 8, pp 339−397, Plenum Press, New York.
37. Fiori, W. R., and Millhauser, G. L. (1995) *Biopolymers 37*, 243−250.

38. Lesk, A. M., and Chothia, C. (1984) *J. Mol. Biol. 174*, 175−191.
39. Gerstein, M., Lesk, A. M., and Chothia, C. (1994) *Biochemistry 33*, 6739−6749.
40. Mowbray, S. L., and Koshland, D. E., Jr. (1987) *Cell 50*, 171−80.
41. Liu, Y., Levit, M., Lurz, R., Surette, M. G., and Stock, J. B. (1997) *EMBO J. 16*, 7231−7240.
42. Danielson, M. A., Biemann, H. P., Koshland, D. E., Jr., and Falke, J. J. (1994) *Biochemistry 33*, 6100−6109.
43. Chervitz, S. A., Lin, C. M., and Falke, J. J. (1995) *Biochemistry 34*, 9722−9733.
44. Lee, G. F., Lebert, M. R., Lilly, A. A., and Hazelbauer, G. L. (1995) *Proc. Natl. Acad. Sci. U.S.A. 92*, 3391−3395.
45. Maruyama, I. N., Mikawa, Y. G., and Maruyama, H. I. (1995) *J. Mol. Biol. 253*, 530−546.
46. Chervitz, S. A., and Falke, J. J. (1995) *J. Biol. Chem. 270*, 24043−24053.
47. Gardina, P. J., and Manson, M. D. (1996) *Science 274*, 425−426.
48. Tatsuno, I., Homma, M., Oosawa, K., and Kawagishi, I. (1996) *Science 274*, 423−425.
49. Ottemann, K. M., and Koshland, D. E., Jr. (1997) *Proc. Natl. Acad. Sci. U.S.A. 94*, 11201−11204.
50. Ogawa, S., and McConnell, H. M. (1967) *Proc. Natl. Acad. Sci. U.S.A. 58*, 19−26.
51. Beth, A. H., Robinson, B. H., Cobb, C. E., Dalton, L. R., Trommer, W. E., Birktoft, J. J., and Park, J. H. (1984) *J. Biol. Chem. 259*, 9717−9728.
52. Anthony-Cahill, S. J., Benfield, P. A., Fairman, R., Wasserman, Z. R., Brenner, S. L., Stafford, W. F. d., Altenbach, C., Hubbell, W. L., and DeGrado, W. F. (1992) *Science 255*, 979−983.
53. Farahbakhsh, Z. T., Hideg, K., and Hubbell, W. L. (1993) *Science 262*, 1416−1419.
54. He, M. M., Voss, J., Hubbell, W. L., and Kaback, H. R. (1997) *Biochemistry 36*, 13682−13687.

BI980305E